Interatomic-Coulombic-decay-induced recapture of photoelectrons in helium dimers

P. Burzynski,[1] F. Trinter,[1] J. B. Williams,[1] M. Weller,[1] M. Waitz,[1] M. Pitzer,[1] J. Voigtsberger,[1] C. Schober,[1] G. Kastirke,[1] C. Müller,[1] C. Goihl,[1] F. Wiegandt,[1] R. Wallauer,[1] A. Kalinin,[1] L. Ph. H. Schmidt,[1] M. Schöffler,[1] G. Schiwietz,[2] N. Sisourat,[3,4] T. Jahnke,[1] and R. Dörner[1,*]

[1]*Institut für Kernphysik, J. W. Goethe-Universität, Max-von-Laue-Strasse 1, 60438 Frankfurt am Main, Germany*

[2]*Helmholtz-Zentrum Berlin für Materialien und Energie, Institute G-ISRR, Hahn-Meitner-Platz 1, 14109 Berlin, Germany*

[3]*Sorbonne Universités, UMR 7614, Laboratoire de Chimie Physique Matière et Rayonnement, F-75005 Paris, France*

[4]*CNRS, UMR 7614, Laboratoire de Chimie Physique Matière et Rayonnement, F-75005 Paris, France*

(Received 11 February 2014; revised manuscript received 5 August 2014; published 25 August 2014)

We investigate the onset of photoionization shake-up-induced interatomic Coulombic decay (ICD) in He_2 at the $He^{+*}(n = 2)$ threshold by detecting two He^+ ions in coincidence. We find this threshold to be shifted towards higher energies compared to the same threshold in the monomer. The shifted onset of ion pairs created by ICD is attributed to a recapture of the threshold photoelectron after the emission of the faster ICD electron.

DOI: 10.1103/PhysRevA.90.022515 PACS number(s): 33.15.Vb, 36.40.Sx

I. INTRODUCTION

Excited ions can get rid of their excess energy via the emission of a photon or an electron. If, however, the excited atom is spatially close to other atoms and the excitation energy is above the ionization threshold of this neighbor, the excess energy can also be transferred to the neighbor, where it leads to emission of an electron. This energy transfer process is called interatomic Coulombic decay (ICD). It was introduced by Cederbaum and coworkers [1] and was demonstrated experimentally first for neon clusters [2] and neon dimers [3]. The related interatomic Auger transitions in solid matter have often been discussed, but broad valence bands, surface and bulk differences, and significant electron energy-loss processes do typically preclude a clear assignment of this process for solids. Many studies have shown since then that ICD is a very general phenomenon occurring in van der Waals–bound (see, e.g., [2–5]) and hydrogen-bound systems (see, e.g., [6–8]). It can be induced by photoionization (see, e.g., [2,3]), photoexcitation [9–12], Auger decay [13,14], ion impact [15–17], and electron impact [18] or, as in the present case, after shake-up [19]. The most extreme system for which ICD has been reported is the helium dimer [20,21]. The neutral He dimer is very weakly bound (about 95 neV), and the internuclear distance extends to very large distances, with a mean distance of about 52 Å. ICD in He_2 can occur when one of the helium atoms is ionized and its remaining electron is shaken up to any excited state [He^{+*} $(n = 2,3,\ldots)$]. In the next step, the He^{+*} $(n = 2)$ He contracts, and during that nuclear motion it undergoes ICD. The electron of the exited He^+ relaxes to the ground state, and the energy is transferred to the neutral neighbor where the ICD electron is emitted. Finally, the two He^+ ions Coulomb explode back to back:

$$\mathrm{He{-}He} \xrightarrow{h\nu} \mathrm{He^{+*} - He} + e_{ph} \xrightarrow{\mathrm{ICD}} \mathrm{He^+ + He^+} + e_{ph} + e_{\mathrm{ICD}}.$$

Usually, ICD and the subsequent Coulomb explosion is discussed in a two-step picture, where the decay is independent from the initial ionization-excitation process. In the present work, we show that close to the ionization-excitation threshold, this two-step approximation breaks down. Photoelectron and ICD electron interaction can lead to recapture of the photoelectron into a bound state of one of the two ions, which quenches the Coulomb explosion. A direct link between the ionization process and ICD has been discussed in two contexts in the literature so far. The first is the recoil effect, where it has been shown experimentally [22] and theoretically [23] that the recoil momentum of the photoelectron or an Auger electron can induce nuclear motion, which in turn modifies the ICD energy spectrum. The second context is closely related to the present work, where Trinter *et al.* [24] have seen a shift of the photoelectron energy due to postcollision interaction (PCI) with the ICD electron [25,26]. In a time-dependent picture the photoelectron is originally created in the potential of a singly charged species. After some delay the ICD electron is emitted, but then it surpasses the slow photoelectron, which from then on feels the attractive potential of a doubly charged ion. This slows down the photoelectron. This streaking towards lower photoelectron energies depends on the time delay between the photoabsorption and the ICD electron and can easily be modeled. It has recently been used to make the first "movie" of nuclear motion during ICD [24]. The same process of postcollision interaction leads, for very small photoelectron energies, to a recapture of a part of the photoelectron wave packet, which is the effect we study here. For atomic Auger decay following inner-shell ionization, PCI is well understood [25,26]. Recently, Schütte *et al.* [27] have experimentally verified the time-dependent picture we have just discussed by showing that the energy exchange between the photoelectron and Auger electron indeed depends on the Auger emission time delay. For atomic multiple ionization, such recapture of the photoelectron by PCI leads to a shifted onset of the production of higher charge states as reported for, e.g., Ar [28,29].

II. EXPERIMENT

The present experiment has been performed at beam line UE112-PGM-1 in the synchrotron radiation facility BESSY (Berlin) during single-bunch operation using a cold-target recoil-ion momentum spectroscopy (COLTRIMS) reaction microscope [30–32]. The photon beam was intersected with a supersonic He gas jet in the center of the COLTRIMS spec-

*doerner@atom.uni-frankfurt.de

trometer. A 7.5 V/cm homogeneous electric field guided the ions towards a position-sensitive microchannel plate detector with hexagonal delay-line readout (RoentDek HEX90) [33]. A nozzle temperature of 21 K at 2.5 bars driving pressure resulted in a fraction of about 1%–2% He_2 in the atomic gas jet. The photon energy was scanned across the He^+ ($n = 2$) threshold. In the offline analysis the momentum vectors of the ions were obtained from the position of impact at the detector and the time of flight. We analyzed ion pairs emitted back to back and the simultaneously measured He^+ ($n = 2$) monomer ions from the atomic helium fraction of the gas jet. The back-to-back events dominate the recoil pair-correlation function slightly above threshold. This fact is related to a small fraction of sequential pair production due to the limited photon density of the energy-filtered synchrotron beam, to an extremely small probability of the correlated electron knock-off transitions close to the threshold, and to a small fraction of secondary ion and atom collisions in the gas jet. He^+ ($n = 2$) ions have been discriminated from the He^+ ($n = 1$) ions by the ion momentum vector (see Fig. 1 in [34]). Close to the He^+ ($n = 2$) threshold,

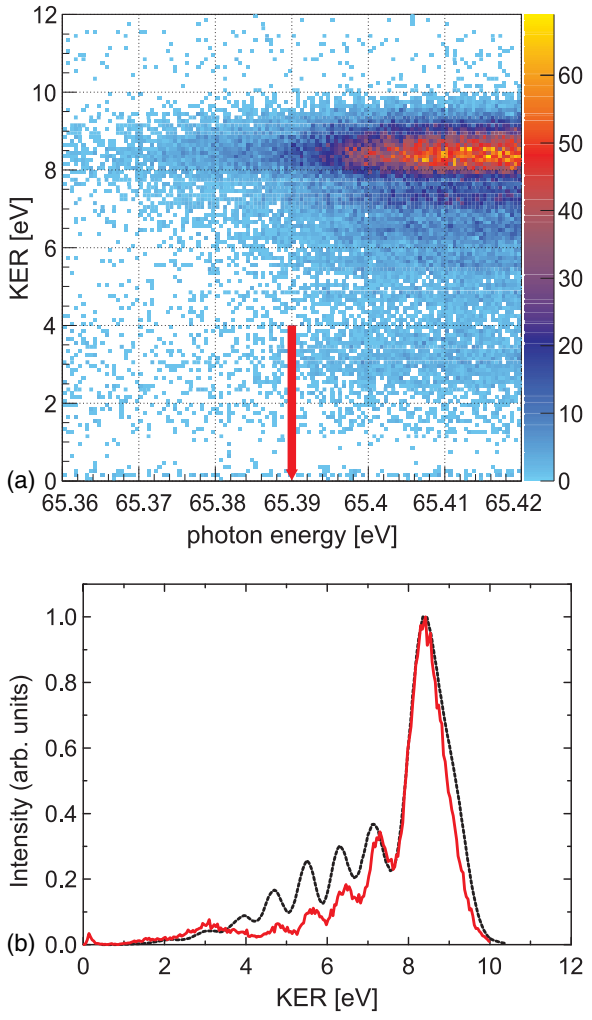

FIG. 1. (Color online) (a) Kinetic energy release (KER) of He^+ ion pairs as a function of photon energy; the red arrow shows the threshold for creating He^{+*} ($n = 2$) for a helium atom. (b) Red solid line: projection of (a) onto the y axis for a photon energy range of 65.41–65.42 eV. Black dotted line: theoretical KER distribution. The two curves are normalized to the maximum.

the He^+ ($n = 1$) ions carry the 1.7 a.u. recoil momentum of the photoelectron while the He^{+*} ($n = 2$) ions are accompanied by a zero-kinetic-energy photoelectron and hence have almost no recoil momentum.

III. RESULTS AND DISCUSSION

Figure 1 shows the measured kinetic energy release (KER; summed over both recoil-ion energies) as function of the photon energy. The KER above the He^{+*} ($n = 2$) threshold [E_γ range of 65.41–65.42 eV; Fig. 1(b)] is in excellent agreement with published work [20]. It shows a vibrational structure from the contracting dimer with a maximum between 8 and 9.5 eV, which results from nuclear wave packet hitting the inner turning point on the potential energy surface of the excited dimer ion (see [21,35] for a detailed analysis).

Figure 2 shows the photon energy dependence of the ion-pair count rate, i.e., a projection of the data from Fig. 1(a) onto the horizontal axis (solid circles) and the count rate from He^{+*} ($n = 2$) monomers (open circles). Both data sets are normalized to the highest-energy point. A constant background for the ion pairs probably resulting from a knock-off process [36,37] and higher harmonics from the beam line has been subtracted.

Owing to the resolution of the beam line, the count rates are not a step function at the He^{+*} ($n = 2$) threshold. The resolution of the beam line is $\sigma = 4.5$ meV, which is extracted from the data of the monomers. These monomers come from atomic helium. The black dashed line in Fig. 2 is a convolution of the step function (black dotted) with a Gaussian function

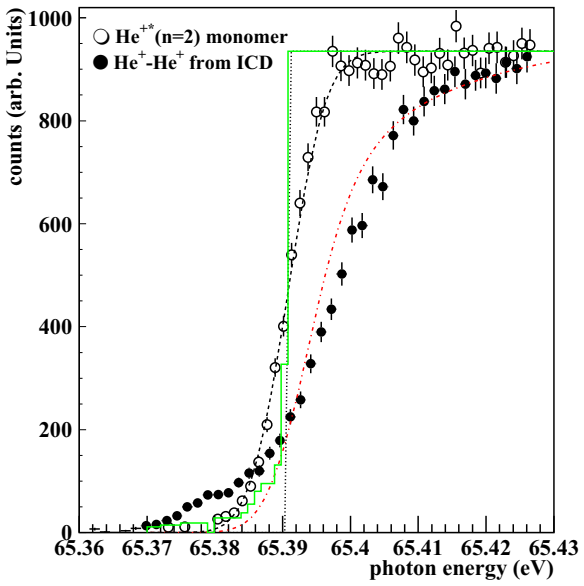

FIG. 2. (Color online) Photon energy dependence of the count rate for two He^+ ions [solid circles; projection of data in Fig. 1(a) onto the x axis] and He^{+*} ($n = 2$) ions from ionization of the monomer (open circles). Black dotted step function: threshold for He^{+*} ($n = 2$); black dashed line: step function convoluted with a Gaussian function ($\sigma = 4.5$ meV) for the energy resolution of the beam line. Green solid line: expected onset of ICD without taking PCI into account (see text); red dash-dotted line: model including recapture of photoelectrons by PCI using calculated widths from Table I (see text) as well as the experimental resolution of $\sigma = 4.5$ meV. The data points are normalized at the highest points.

with a FWHM of 4.5 meV. This line follows the monomer ion count rate very well. The ion-pair count rate shows a significant energy offset compared to the monomers. Note that monomers and ion pairs are measured simultaneously in our setup, which excludes any possible systematic error on the photon energy as the origin of this energy offset. We will show now that the shifted onset of the ion-pair production is caused by recapture of the slow near-threshold photoelectron after ICD, which neutralizes one of the two ions. A classical modeling of this recapture process, summing over all calculated ICD channels using calculated ICD lifetimes, results in the dash-dotted red line in Fig. 2, which nicely reproduces the shifted onset. There are no free parameters in this calculation. The model is presented in the following.

In the present data, the photoelectron energy is below 50 meV, while the ICD electron has an energy of 6–15 eV. Even though there is a time delay t_{ICD} between the emission of the photoelectron and ICD electron, the ICD electron will always overtake the photoelectron in the vicinity of the residual ion(s) because t_{ICD} is small and the ICD electron is much faster than the photoelectron.

Note that t_{ICD} is not the lifetime of the respective ICD channel but the time at which ICD occurs for this individual event. For the present case the travel time of the ICD electron is negligible compared to t_{ICD}. The photoelectron therefore starts making its way to the continuum, initially leaving behind a singly charged species. However, when the ICD electron is emitted, the ion charge state increases from singly to doubly charged, which changes the potential the photoelectron feels, at least after it has been overtaken by the ICD electron, from $-1/r_e$ to $-2/r_e$ (in atomic units), where r_e is the distance the photoelectron has reached at time t_{ICD}.

We calculate the trajectory of the photoelectron classically by starting the electron at a distance r_{es} in a Coulomb potential with an initial kinetic energy $E_\gamma - E_{\mathrm{IPX}} + 1/r_{es}$, where E_γ is the photon energy and E_{IPX} is the ionization potential of He plus the energy it takes to excite He^+ from its ground state to He^{+*} ($n = 2$). We have chosen $r_{es} = 10$ a.u. and have verified that the results are insensitive to this choice over a wide range. Without the ICD electron the photoelectron would escape to the continuum. However, if ICD occurs, the electron loses the energy $-1/r_e$ and might get trapped in the ionic potential. For every particular electronic and vibrational He^{+*} ($n = 2$) He state ICD occurs with an exponential time dependence. We calculate the fraction of recapture photoelectrons using this exponential distribution of t_{ICD} for each photon energy. We then sum over all electronic and vibrational states. The electronic states are weighted with their statistical weight, and

TABLE I. Calculated characteristics of the He^{+*} ($n = 2$) He states: Franck-Condon factors for the overlap with the He_2 ground state, vibrational-state energies, and ICD lifetimes [35]. Dissociation limit is 65.393 eV.

v	$^2\Sigma_g^+ : 2p_z,2s$	$^2\Sigma_u^+ : 2p_z,2s$	$^2\Pi_g : 2p_{x,y}$	$^2\Pi_u : 2p_{x,y}$
		Franck-Condon factors		
0	7.25×10^{-5}	2.95×10^{-5}	5.34×10^{-6}	1.70×10^{-5}
1	3.85×10^{-4}	2.11×10^{-4}	5.47×10^{-5}	1.39×10^{-4}
2	1.55×10^{-3}	9.40×10^{-4}	3.15×10^{-4}	6.80×10^{-4}
3	4.56×10^{-3}	2.91×10^{-3}	1.29×10^{-3}	2.39×10^{-3}
4	7.31×10^{-3}	6.20×10^{-3}	4.34×10^{-3}	7.26×10^{-3}
5	3.30×10^{-2}	2.10×10^{-2}	1.26×10^{-2}	2.06×10^{-2}
6	2.72×10^{-2}	1.82×10^{-2}	3.16×10^{-2}	5.30×10^{-2}
7	4.92×10^{-2}	1.36×10^{-1}	8.86×10^{-2}	1.88×10^{-1}
8	3.13×10^{-1}	1.20×10^{-1}	3.88×10^{-1}	-
		Lifetimes (fs)		
0	30.61	33.49	34.08	22.00
1	37.40	36.44	38.25	27.15
2	51.89	49.00	47.43	39.27
3	81.07	69.58	66.06	61.22
4	147.10	113.76	111.16	127.44
5	377.19	261.05	251.72	387.04
6	1420	957.02	839.12	1810
7	1975	2640	4560	15 570
8	24 690	8710	53 960	
		Negative shifts of the vibrational level compared to the monomer (eV)		
0	1.24×10^{-1}	1.45×10^{-1}	1.68×10^{-1}	1.43×10^{-1}
1	8.01×10^{-2}	9.36×10^{-2}	1.13×10^{-1}	9.09×10^{-2}
2	4.61×10^{-2}	5.72×10^{-2}	6.95×10^{-2}	5.19×10^{-2}
3	2.38×10^{-2}	3.09×10^{-2}	3.79×10^{-2}	2.58×10^{-2}
4	1.06×10^{-2}	1.45×10^{-2}	1.74×10^{-2}	1.07×10^{-2}
5	4.13×10^{-3}	5.94×10^{-3}	6.40×10^{-3}	3.34×10^{-3}
6	9.09×10^{-4}	1.50×10^{-3}	1.70×10^{-3}	6.75×10^{-4}
7	7.03×10^{-5}	3.75×10^{-4}	2.35×10^{-4}	4.37×10^{-5}
8	5.35×10^{-5}	1.48×10^{-5}	2.99×10^{-6}	

the vibrational states are weighted with their Franck-Condon overlap with the He_2 ground state. Franck-Condon factors, energies, and ICD lifetimes for each state are given in Table I.

There are two counteracting effects included in this calculation. First, the threshold for each state He^{+*} ($n = 2$) He will be slightly below the He^{+*} ($n = 2$) threshold for the monomer because of the larger size of the combined electronic potential due to both heavy constituents of the dimer (see Table I for binding energies). Thus, neglecting the recapture, the threshold for ion-pair creation would be slightly smeared to lower energies, as shown by the solid green curve in Fig. 2. If one includes the recapture as described above, the solid green curve is modified to the dash-dotted red curve in Fig. 2, which is shifted towards higher photon energies. This dash-dotted red curve also includes the photon energy resolution which we obtained *in situ* from the monomer. This calculation captures the main effect seen in the experiment. Experimentally, we also see a small contribution of ion pairs below threshold, which is not reproduced by our calculation. The origin of these contributions below threshold is unclear but might be related to details of the angular distribution of ejected ICD and photoelectrons or to the accuracy of the computed negative energy shift.

IV. CONCLUSIONS

In conclusion, we have shown that close-to-threshold fragment creation by ICD cannot be treated independently of the ionization process. Postcollision interaction of the photoelectron with the ICD electron can even lead to recapture of the photoelectron. This observed effect is similar to PCI between photoelectron and fast Auger electrons in atomic species. While we have studied only the monopole term of this postcollision here, we expect that the angular distributions of the electrons will also be altered, an effect studied recently for the atomic Auger case [26]. The discussed recapture will also be active at the threshold for creation of He^{+*} in $n = 3$ and higher. In this case the angular distributions of photoelectron and ICD electron will be different (see [38]). We believe that PCI in the continuum will, in the future, become a major tool for ultrafast time-resolved studies, as shown recently in pioneering work by Trinter *et al.* [24].

ACKNOWLEDGMENTS

We thank the staff of BESSY II for experimental support. This work was funded by the Deutsche Forschungsgemeinschaft and supported by RoentDek Handels GmbH.

[1] L. S. Cederbaum, J. Zobeley, and F. Tarantelli, Phys. Rev. Lett. **79**, 4778 (1997).
[2] S. Marburger, O. Kugeler, U. Hergenhahn, and T. Möller, Phys. Rev. Lett. **90**, 203401 (2003).
[3] T. Jahnke, A. Czasch, M. S. Schöffler, S. Schössler, A. Knapp, M. Käsz, J. Titze, C. Wimmer, K. Kreidi, R. E. Grisenti, A. Staudte, O. Jagutzki, U. Hergenhahn, H. Schmidt-Böcking, and R. Dörner, Phys. Rev. Lett. **93**, 163401 (2004).
[4] G. Öhrwall, M. Tchaplyguine, M. Lundwall, R. Feifel, H. Bergersen, T. Rander, A. Lindblad, J. Schulz, S. Peredkov, S. Barth, S. Marburger, U. Hergenhahn, S. Svensson, and O. Björneholm, Phys. Rev. Lett. **93**, 173401 (2004).
[5] T. Ouchi, K. Sakai, H. Fukuzawa, X.-J. Liu, I. Higuchi, Y. Tamenori, K. Nagaya, H. Iwayama, M. Yao, D. Zhang, D. Ding, A. I. Kuleff, S. D. Stoychev, Ph. V. Demekhin, N. Saito, and K. Ueda, Phys. Rev. Lett. **107**, 053401 (2011).
[6] I. B. Müller and L. S. Cederbaum, J. Chem. Phys. **125**, 204305 (2006).
[7] T. Jahnke, H. Sann, T. Havermeier, K. Kreidi, C. Stuck, M. Meckel, M. Schöffler, N. Neumann, R. Wallauer, S. Voss, A. Czasch, O. Jagutzki, A. Malakzadeh, F. Afaneh, Th. Weber, H. Schmidt-Böcking, and R. Dörner, Nat. Phys. **6**, 139 (2010).
[8] M. Mucke, M. Braune, S. Barth, M. Förstel, T. Lischke, V. Ulrich, T. Arion, U. Becker, A. Bradshaw, and U. Hergenhahn, Nat. Phys. **6**, 143 (2010).
[9] F. Trinter, J. B. Williams, M. Weller, M. Waitz, M. Pitzer, J. Voigtsberger, C. Schober, G. Kastirke, C. Müller, C. Goihl, P. Burzynski, F. Wiegandt, R. Wallauer, A. Kalinin, L. Ph. H. Schmidt, M. S. Schöffler, Y.-C. Chiang, K. Gokhberg, T. Jahnke, and R. Dörner, Phys. Rev. Lett. **111**, 233004 (2013).
[10] A. Golan and M. Ahmed, J. Phys. Chem. Lett. **3**, 458 (2012).
[11] K. Gokhberg, A. B. Trofimov, T. Sommerfeld, and L. S. Cederbaum, Europhys. Lett. **72**, 228 (2005).
[12] B. Najjari, A. B. Voitkiv, and C. Müller, Phys. Rev. Lett. **105**, 153002 (2010).
[13] R. Santra and L. S. Cederbaum, Phys. Rev. Lett. **90**, 153401 (2003).
[14] K. Kreidi *et al.*, Phys. Rev. A **78**, 043422 (2008).
[15] H. K. Kim *et al.*, Proc. Natl. Acad. Sci. U.S.A. **108**, 11821 (2011).
[16] H. K. Kim, H. Gassert, M. S. Schöffler, J. N. Titze, M. Waitz, J. Voigtsberger, F. Trinter, J. Becht, A. Kalinin, N. Neumann, C. Zhou, L. Ph.H. Schmidt, O. Jagutzki, A. Czasch, H. Merabet, H. Schmidt-Böcking, T. Jahnke, A. Cassimi, and R. Dörner, Phys. Rev. A **88**, 042707 (2013).
[17] J. Titze *et al.*, Phys. Rev. Lett. **106**, 033201 (2011).
[18] S. Yan, P. Zhang, X. Ma, S. Xu, B. Li, X. L. Zhu, W. T. Feng, S. F. Zhang, D. M. Zhao, R. T. Zhang, D. L. Guo, and H. P. Liu, Phys. Rev. A **88**, 042712 (2013).
[19] T. Jahnke, A. Czasch, M. Schöffler, S. Schössler, M. Käsz, J. Titze, K. Kreidi, R. E. Grisenti, A. Staudte, O. Jagutzki, L. Ph. H. Schmidt, Th. Weber, H. Schmidt-Böcking, K. Ueda, and R. Dörner, Phys. Rev. Lett. **99**, 153401 (2007).
[20] T. Havermeier, T. Jahnke, K. Kreidi, R. Wallauer, S. Voss, M. Schöffler, S. Schössler, L. Foucar, N. Neumann, J. Titze, H. Sann, M. Kühnel, J. Voigtsberger, J. H. Morilla, W. Schöllkopf, H. Schmidt-Böcking, R. E. Grisenti, and R. Dörner, Phys. Rev. Lett. **104**, 133401 (2010).
[21] N. Sisourat, N. V. Kryzhevoi, P. Kolorenc, S. Scheit, T. Jahnke, and L. S. Cederbaum, Nat. Phys. **6**, 508 (2010).
[22] K. Kreidi *et al.*, Phys. Rev. Lett. **103**, 033001 (2009).

[23] Ph. V. Demekhin, S. Scheit, and L. S. Cederbaum, J. Chem. Phys. **131**, 164301 (2009).
[24] F. Trinter, J. B. Williams, M. Weller, M. Waitz, M. Pitzer, J. Voigtsberger, C. Schober, G. Kastirke, C. Müller, C. Goihl, P. Burzynski, F. Wiegandt, T. Bauer, R. Wallauer, H. Sann, A. Kalinin, L. Ph. H. Schmidt, M. Schöffler, N. Sisourat, and T. Jahnke, Phys. Rev. Lett. **111**, 093401 (2013).
[25] A. Russek and W. Mehlhorn, J. Phys. B **19**, 911 (1986).
[26] A. L. Landers, F. Robicheaux, T. Jahnke, M. Schöffler, T. Osipov, J. Titze, S. Y. Lee, H. Adaniya, M. Hertlein, P. Ranitovic, I. Bocharova, D. Akoury, A. Bhandary, Th. Weber, M. H. Prior, C. L. Cocke, R. Dörner, and A. Belkacem, Phys. Rev. Lett. **102**, 223001 (2009).
[27] B. Schütte, S. Bauch, U. Frühling, M. Wieland, M. Gensch, E. Plönjes, T. Gaumnitz, A. Azima, M. Bonitz, and M. Drescher, Phys. Rev. Lett. **108**, 253003 (2012).
[28] J. A. R. Samson, W. C. Stolte, Z. X. He, J. N. Cutler, and D. Hansen, Phys. Rev. A **54**, 2099 (1996).
[29] R. Guillemin, S. Sheinerman, C. Bomme, L. Journel, T. Marin, T. Marchenko, R. K. Kushawaha, N. Trcera, M. N. Piancastelli, and M. Simon, Phys. Rev. Lett. **109**, 013001 (2012).
[30] J. Ullrich, R. Moshammer, A. Dorn, R. Dörner, L. Ph. Schmidt, and H. Schmidt-Böcking, Rep. Prog. Phys. **66**, 1463 (2003).
[31] R. Dörner, V. Mergel, O. Jagutzki, L. Spielberger, J. Ullrich, R. Moshammer, and H. Schmidt-Böcking, Phys. Rep. **330**, 95 (2000).
[32] T. Jahnke, Th. Weber, T. Osipov, A. L. Landers, O. Jagutzki, L. Ph. H. Schmidt, C. L. Cocke, M. H. Prior, H. Schmidt-Böcking, and R. Dörner, J. Electron Spectrosc. Relelat. Phenom. **141**, 229 (2004).
[33] O. Jagutzki, A. Cerezo, A. Czasch, R. Dörner, M. Hattass, M. Huang, V. Mergel, U. Spillmann, K. Ullmann-Pfleger, Th. Weber, H. Schmidt-Böcking, and G. D. W. Smith, IEEE Trans. Nucl. Sci. **49**, 2477 (2002).
[34] R. Dörner *et al.*, Phys. Rev. Lett. **76**, 2654 (1996).
[35] N. Sisourat, N. V. Kryzhevoi, P. Kolorenč, S. Scheit, and L. S. Cederbaum, Phys. Rev. A **82**, 053401 (2010).
[36] T. Havermeier, T. Jahnke, K. Kreidi, R. Wallauer, S. Voss, M. Schöffler, S. Schössler, L. Foucar, N. Neumann, J. Titze, H. Sann, M. Kühnel, J. Voigtsberger, A. Malakzadeh, N. Sisourat, W. Schöllkopf, H. Schmidt-Böcking, R. E. Grisenti, and R. Dörner, Phys. Rev. Lett. **104**, 153401 (2010).
[37] H. Ni, C. Ruiz, R. Dörner, and A. Becker, Phys. Rev. A **88**, 013407 (2013).
[38] T. Havermeier, K. Kreidi, R. Wallauer, S. Voss, M. Schöffler, S. Schössler, L. Foucar, N. Neumann, J. Titze, H. Sann, M. Kühnel, J. Voigtsbeger, N. Sisourat, W. Schöllkopf, H. Schmidt-Böcking, R. E. Gristenti, R. Dörner, and T. Jahnke, Phys. Rev. A **82**, 063405 (2010).